Thermodynamic stability of the UO$_2$ surfaces: Interplay between over-stoichiometry and polarity compensation

François Bottin[*] and Grégory Geneste[†]

CEA, DAM, DIF, F-91297 Arpajon, France

Gérald Jomard[‡]

CEA, DEN, DEC, F-13108 Saint-Paul-lez-Durance, France

The thermodynamic stability of UO$_2$ surfaces is investigated using *ab initio* calculations. We employ the GGA+U framework to properly model the strong electronic correlations of the uranium 5f electrons. Among the seven terminations of the (100), (110), and (111) orientations studied in this paper, we predict that the stoichiometric O-(111) is the most stable one under oxygen-poor or -intermediary environments. At odds with other fluorite surfaces, the overstoichiometric and polar O$_2$-(100) and O$_2$-(111) terminations become the most stable in oxygen-rich environments. For the latter, strong modifications of the electronic structure appear within the upper layers, in order to fulfill the polarity compensation criterion. Some U-5f states are emptied, leading to higher oxidation 5+ and 6+ states for uranium in the outermost layers, but leaving the surface insulating. This unexpected polarity compensation mechanism is not observed for other charge transfer compounds (such as PuO$_2$) and can be related to the f-f Mott-Hubbard band gap of the UO$_2$ material. By considering the most stable stoichiometric and overstoichiometric terminations, the Castell's ratio can be fulfilled, explaining the Wulff shape of nanovoids in UO$_2$ crystals.

I. INTRODUCTION

For several decades, uranium oxides have attracted a large interest owing to their role in the nuclear industry (as nuclear reactor fuels or for very long term storage of spent fuels from actinides). From this perspective, a lot of work concerns the safety and integrity of nuclear fuel rods or the corrosion of actinide materials in extreme chemical and thermodynamic environments [1]. Thus, the UO$_2$ surfaces [2,3] as well as their interaction with various chemical species [4–9] (hydrogen, oxygen, water...) have been extensively studied for a long time by theoretical as well as experimental tools.

Beyond technological or environmental issues, significant attention has focus on actinide oxides for theoretical reasons. The behavior of the f electrons in actinide-based materials is complex and often implies the need to go beyond a standard description of the electronic structure. In particular, the density functional theory (DFT) within its standard exchange-correlation approximations (LDA, GGA) fails to describe UO$_2$ as an insulator and does not capture the behavior of the strongly correlated f electrons. In the DFT framework, the correct band gap as well as other features of the f electrons can be recovered using an additional term called the Hubbard U parameter and related to the intra-atomic Coulomb interaction [10–12]. For example, at a very early stage of this approach, the bulk and surface electronic properties of the UO$_2$ compound have been successfully described using this method [13]. Even if some difficulties were highlighted when the DFT+U method has been demonstrated over time, particular challenges have been

circumvented and the method is now proven to give reliable results for actinide oxides [14–16].

In previous studies concerning actinide dioxides, it was shown that the use of DFT+U is not only mandatory to obtain a correct description of the bulk properties [14,15,17] but also to capture the relative stability of the various surfaces [18]. For instance, consider PuO$_2$, standard DFT leads to an unexpected stabilization of two overstoichiometric polar terminations in oxygen rich environments, the O$_2$-(111) and O$_2$-(100) ones. When using DFT+U, these latter terminations are destabilized with respect to the stoichiometric O-(111) and O-(100) surfaces, leading to the following energetic stability sequence $\sigma_{111} < \sigma_{110} < \sigma_{100}$, in agreement with what is currently expected for insulators having the fluorite structure [19] and exposing polar/nonpolar terminations [20,21].

More recently, the calculation of the UO$_2$ surface energy has attracted much interest using interatomic potentials [22–24] as well as by means of *ab initio* simulations [19,25–31]. The results found by the authors disclosed a serious issue: The convergence of the surface energy as a function of the slab thickness is sometimes questionable. In addition, the previous difficulties encountered at the bulk calculation level, which where considered as definitively solved, seems to play an important role again when performing surface simulations. On one hand, one could ask, are they responsible for the strong discrepancies existing between some theoretical results? On the other hand, an important disagreement still remains with experiments concerning the surface energy ratio between (100) and (111) terminations. Studying the Wulff shape of nanovoids in UO$_2$ crystals, by means of scanning electron microscopy, Castell [32] found that this ratio is equal to $\frac{\sigma_{100}}{\sigma_{111}} = 1.42 \pm 0.05$. In view of the difficulties faced by computational scientists to find the UO$_2$ surface energies, this quantity became a reference to judge the results found [33,34]. However, by performing calculations on stoichiometric terminations, no conclusive

---

*francois.bottin@cea.fr

†gregory.geneste@cea.fr

‡gerald.jomard@cea.fr

finding had been obtained, the ratio being at most in the 1.8–2.0 range in all theoretical works. Does this discrepancy with experiments come from other nonstoichiometric terminations not yet considered in computational studies?

In this paper, we present the electronic structure and thermodynamic stability of various terminations of the (100), (110), and (111) orientations of UO_2. In addition to the stoichiometric ones frequently studied in other works, we also focus on some nonstoichiometric terminations not previously reported. In the computational part we propose a systematic scheme that will guarantee convergence of the surface energy with respect to the slab thickness. Concerning results, we find that the surface energies of some nonstoichiometric terminations can be strongly affected by external chemical environments and be more stable than stoichiometric ones. We thus show that a correct treatment of both stoichiometric and nonstoichiometric terminations is critical (i) to have a comprehensive understanding of the thermodynamic stability of UO_2 surfaces and (ii) to explain the shape of nanovoids in UO_2, since the Castell's ratio is then fulfilled. We finish by highlighting the effects coming from the electronic structure and the reasons why, in contrast to PuO_2 behavior, the nonstoichiometric terminations can be stabilized in the case of the Mott-Hubbard insulator UO_2.

II. COMPUTATIONAL DETAILS

A. *Ab initio* calculations

At polar surfaces, both atomic relaxations and strong electronic modifications are expected to play a significant role. In this paper, we thus choose to treat electronic and atomic structures on equal footing by using *ab initio* calculations. These simulations are based on density functional theory [35,36] (DFT) and performed using the ABINIT [37,38] package in the framework of the projector augmented wave [39,40] (PAW) method. The generalized gradient approximation (GGA) is adopted for the exchange and correlation functional, following the form proposed by Perdew, Burke, and Ernzerhof (PBE) [41] and as implemented in the LIBXC library [42].

We use the same oxygen PAW atomic dataset as the one employed in our previous works [14,18,43] and build our own uranium PAW atomic dataset using the ATOMPAW generation code [44]. The latter is generated using the $6s^2 6p^6 7s^2 6d^2 5f^2$ electronic configuration, with 14 valence electrons and a PAW sphere radius equal to 1.1 Å. In order to achieve an accuracy equal to or better than 1 meV for total energies per formula unit (see below for reasons), the cutoff energy is chosen to be 25 Ha. Structural optimizations are performed using the Broyden-Fletcher-Goldfarb-Shanno minimization scheme until the maximal cartesian component of the atomic forces is below 1.0×10^{-4} Ha/Bohr (≈ 0.005 eV/Å). The calculations have been carried out using a triple parallelization level as implemented in the ABINIT code [45].

To ensure that the insulating ground state of UO_2 is correctly reproduced, the Hubbard scheme (GGA+U) has been employed [46] with the $U = 4.5$ eV and $J = 0.5$ eV parameters. Employing this on-site Hubbard interaction, we found a band gap and a lattice parameter for UO_2 equal to $\Delta = 2.5$ eV and $a_0 = 5.54$ Å, respectively, in good agreement
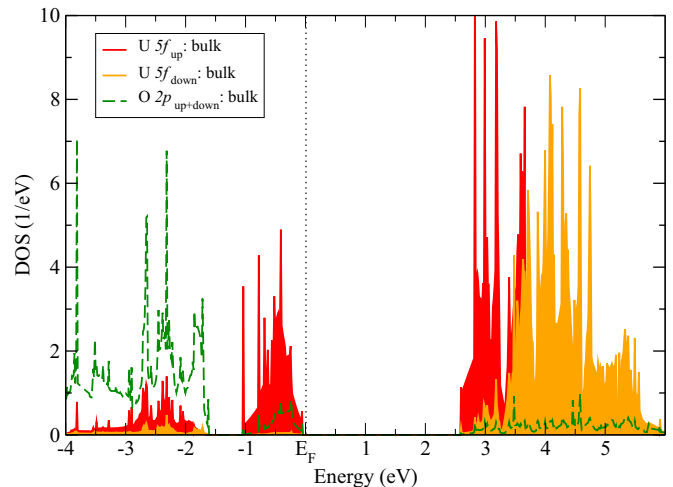

FIG. 1. Electronic density of states of UO_2 in the framework of DFT+U calculations. E_F is set at the VBM, just above the lower filled (and narrow) Hubbard band. The upper emptied (and wide) Hubbard band is 2.5 eV above.

with previous theoretical (see Table 2 of Ref. [47]) and experimental [48–50] ($a_0 = 5.47$ Å and $\Delta \approx 2.1$ eV) results. The distribution of electronic states is also well reproduced (see Fig. 1) with, in particular, some filled U-$5f$ states above the O-$2p$ valence band, just below the Fermi level (E_F), and others emptied U-$5f$ states above E_F. This is the picture previously obtained by means of two experimental techniques [49]: (i) X-ray photoemission spectroscopy shows a clear evidence for the localization of the $5f$ electrons (the filled $^2F_{5/2}$ and $^2F_{7/2}$ states below E_F), and (ii) Bremsstrahlung Isochromat Spectroscopy assigns the empty states just above E_F to $^4I_{9/2}$ and $^4I_{11/2}$. Contrary to charge transfer band gap materials, the UO_2 band gap is thus composed of cationic states at both valence band maximum (VBM) and conduction band minimum (CBM) and presents a Mott-Hubbard f-f band gap. This feature will be very important, when discussing the properties of UO_2 surfaces below. Spin-orbit (SO) coupling and noncollinear magnetism are not considered in the present calculations, although the SO effect might be non-negligible in actinide compounds. However, the typical ratio between Coulomb repulsion and SO in actinide compounds with unfilled $5f$ shells is 1000-10000:300 [51], showing that the primary effect to consider and to correctly model is the electron correlation.

B. Slab and surface

Atomic and electronic structures of the terminations are obtained through supercell calculations in the framework of the slab model. The convergence of surface properties with respect to the number of planes is carefully checked (see Sec. III A) in order to ensure that (i) the two terminations of the slab are independent and (ii) the bulk properties are recovered at the center of the slab. High precision is still required from this perspective.

Three preferential orientations of the actinide dioxide crystals AnO_2 are generally studied: the (110), (100), and (111) ones. The (110) orientation, composed of neutral AnO_2
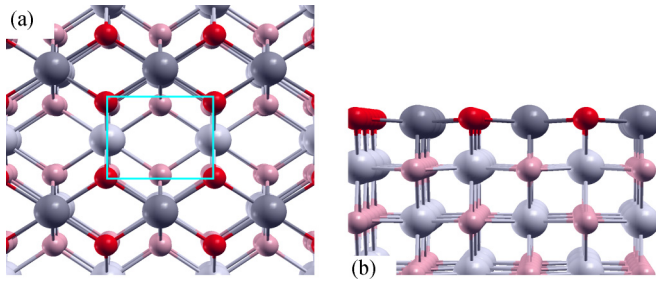
FIG. 2. Left (right) panel: Top (side) view of the UO$_2$-(110) nonpolar and stoichiometric termination.

planes (in the ionic limit), is called nonpolar (see Fig. 2). Conversely, the (100) and (111) orientations are named polar since they present a stacking sequence of charged O$_2$ and An planes [20,21] (see Figs. 3 and 4). In the ionic limit, assuming that the charge of oxygen and uranium atoms are -2 and $+4$, respectively, each plane bears a ±4 charge. This stacking leads to a divergence of the electrostatic potential which can only be healed by a modification of the surface charge. For UO$_2$, the polarity compensation criterion is achieved if the surface charge is equal to ±2. This can be carried out through a modification of the surface stoichiometry or a modification of the surface electronic structure. The former case corresponds to the O-(111) or O-(100) terminations, for
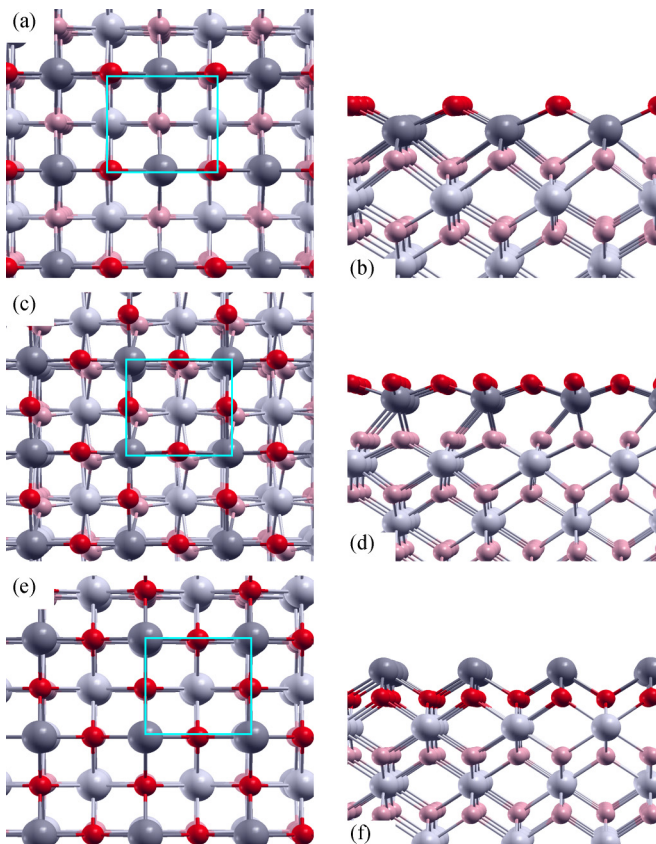

FIG. 3. Left (right) panel: Top (side) view of the stoichiometric O-(100) [see (a) and (b)], overstoichiometric O$_2$-(100) [see (c) and (d)] and understoichiometric U-(110) [see (e) and (f)] polar terminations.
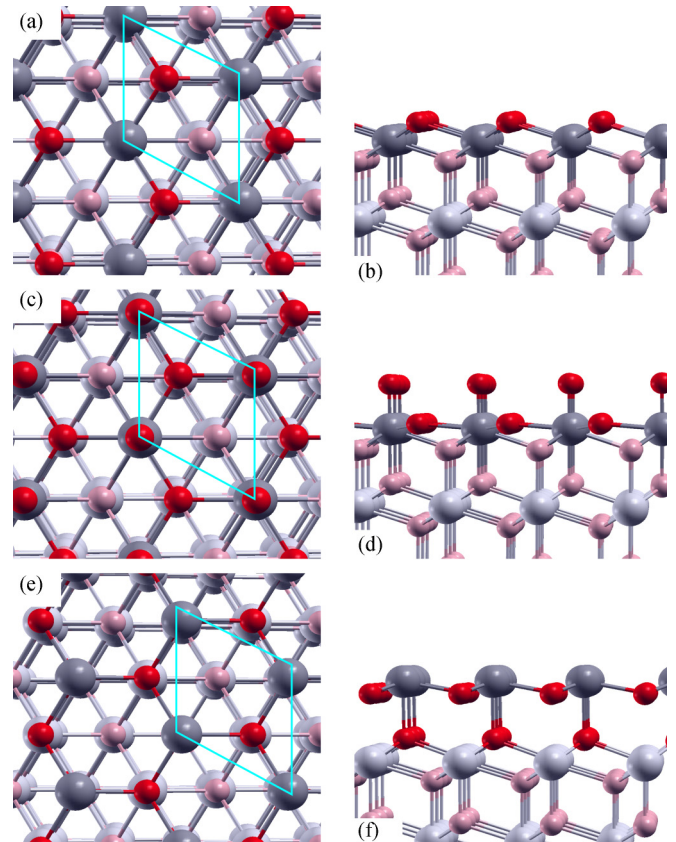

FIG. 4. Left (right) panel: Top (side) view of the stoichiometric O-(111) [see (a) and (b)], overstoichiometric O$_2$-(111) [see (c) and (d)] and understoichiometric U-(111) [see (e) and (f)] polar terminations.

which the polarity compensation criterion is naturally fulfilled (in the following, the stoichiometric polar terminations are called stoichiometric because the slab contains an entire number of UO$_2$ formula units). The latter case arises when oxygen or uranium atoms are in excess on the surface (the over- or understoichiometric terminations, respectively). Generally, stoichiometric (non)polar terminations are expected to be more stable than under- or overstoichiometric polar ones [20,21]. The energetic cost of a modification of the surface electronic structure is considered to be higher than the one corresponding to a modification of the surface stoichiometry.

In this paper, we compare the properties (electronic structure, thermodynamic stability) of three stoichiometric terminations, the nonpolar UO$_2$-(110) and polar O-(100) and O-(111) ones, with four nonstoichiometric terminations. For each of both the (100) and (111) polar orientations, two other terminations are studied: the understoichiometric U-(100) and U-(111) (formed by removing one oxygen atom from the O termination) and the overstoichiometric O$_2$-(100) and O$_2$-(111) (formed by adding one oxygen atom on the O termination). Thus, seven terminations are studied in the following (see Figs. 2, 3, and 4).

Different **k**-point grid meshes are employed during the calculations according to the orientations. To keep approximately the same **k**-point density, irrespective of the terminations, we use the $2 \times 4 \times 4$, $2 \times 3 \times 4$ and $2 \times 4 \times 4$ Monkhorst-Pack meshes [52] for the (100), (110), and (111) terminations,

respectively. The magnetic structure of UO_2 is chosen as antiferromagnetic, with U atoms ferromagnetically coupled inside each plane parallel to the surface, and these planes antiferromagnetically coupled with each other.

C. Metastable states

It is now well established that DFT$+U$ leads to the appearance of electronic metastable states. Without close monitoring, self-consistent DFT$+U$ calculations might converge to a state that is not the ground state of the system, especially when the correlated electrons are f electrons. These metastable states differ from each other by the occupation matrices (OM) of the correlated orbitals (U $5f$ in our case). Two schemes named "Occupation Matrix Control" (OMC) [14,15,17] and "U-ramping" [16] have been demonstrated to overcome this problem. In the present paper, we use the first method proposed to ensure that the true ground state is reached in each configuration studied.

Another approach has been proposed recently [53]. Authors take benefit of the valuable information contained in the large number of metastable states and build a model Hamiltonian able to find the correct ground state of the crystal. In particular, when applied to UO_2, the authors find the correct ground state with the 3**k** AFM magnetic structure.

In OMC, the real ground state of the material is obtained by exploring, as much as possible, the metastable states. This exploration is performed as follows: by (i) building all the n OM corresponding to the combinations of the f state occupations (diagonal in the system of axis used, and with f states either full or empty), (ii) performing n calculations using each of them as starting points, (iii) keeping the OM constant along the electronic structure minimization (during 20 steps) and releasing the constraint to converge for each calculation, and finally (iv) selecting the lowest (ground) state among the n results. For instance, in the case of UO_2, the 7 high-spin (in order to verify the Hund's first rule) f orbitals have to be filled by 2 electrons. This choice of 2 states among 7 available corresponds to a C_2^7 combination and 21 OM constructed in all.

In general, the OMC scheme is considered to be sufficient to obtain the ground state of a system in DFT$+U$ calculations. However, several additional remarks, generally not explained or not taken into account, can be very useful in at this point:

(a) First, for surface calculations, the OM of the ground state is required to start the self-consistent field (SCF) process. Consequently, this OM has to be found beforehand at the level of bulk calculations. If various orientations of the slab are considered, the OM has to be expressed in the correct basis of each orientation. The scheme proposed above being very time consuming (and tedious), the search of the OM of the ground state is generally carried out once on a bulk reference cell (for example: an AFM unit cell with 2 uranium and 4 oxygen atoms in the present calculations). Then, the ground state OM is expressed for other orientations by performing a basis transformation. In this paper, we perform an independent search for each orientation, in other word, on various superbulks (with more formula units as previously) exhibiting the (100), (110), and (111) stacking sequence of planes. The energy difference found between their ground

states is equal to 3 mHa/f.u. approximately. This result has many serious consequences: This means that the true ground state is not or never achieved and that no reference energy can be safely used for surface energy calculations.

(b) Thus, it is also strongly advised to turn off the crystal symmetries for both bulk and slab calculations. Doing that, the three previous ground states are then lowered and separated by less than 1 meV/f.u., a difference equal to the error induced by other numerical parameters (**k** points, cutoff energy...).

(c) Moreover, when performing atomic relaxation, it is needed to fix the OM at the beginning of each SCF cycle. For each new set of atomic positions, the electronic starting point may be far away from the fixed point of the previous minimization process. Consequently, the SCF cycle may not converge or exit from the global minimum and converge towards a local minimum. By reimposing the OM of the ground state at the beginning of each SCF cycle, the convergence is easier and safer.

(d) Finally, at these conditions, an efficient Kohn-Sham equations block eigensolver is needed to converge each step of the SCF cycle. Indeed, when the symmetries are broken, the SCF cycle encounters a large number of degrees of freedom: up to 18 **k** points, two spin channels, a large number of f electrons around the Fermi level... In this paper, we employ the efficient LOBPCG eigensolver [45], as implemented in the ABINIT code, using an increased block size and line minimization with respect to other more standard calculations.

To summarize, in order to be confident in a ground state, used thereafter as a reference in slab and surface calculations, it is strongly advised to switch off the symmetries, compute the reference bulk system (OM, the bulk total energy $E_{\mathrm{bulk}}^{UO_2}$...) for one superbulk and use the OM obtained for the ground state to start each SCF of the atomic relaxation process. We highlight that the effort is only performed once at the bulk calculation level and no longer at the surface calculation level. Consequently, the overall computational time spent using the "Occupation Matrix Control" (OMC) would be lower than for the "U-ramping" scheme, for which the effort has to be made at each new calculation (bulk, surface...) [19,29].

III. UO_2 SURFACES

A. The surface energy

Using this bulk reference energy $E_{\mathrm{bulk}}^{UO_2}$, we can safely compute, for the stoichiometric systems, the surface energy of the seven terminations i as:

$$E_{\mathrm{surf}}^i = \tfrac{1}{2}\big[E_{\mathrm{slab}}^i - N_{UO_2} E_{\mathrm{bulk}}^{UO_2}\big] \tag{1}$$

with N_{UO_2} the number of UO_2 formula units in the slab. In order to prove that the bulk ground state is really obtained, we compute the difference of the surface energies $\Delta E = (E_{\mathrm{surf}}^i(N_{UO_2}) - E_{\mathrm{surf}}^i(\infty))/E_{\mathrm{surf}}^i(\infty)$ with respect to the number of formula units in the slab (with ∞ corresponding to the maximum number of planes considered for each slab). The convergence of this quantity is displayed in Fig. 5 for stoichiometric terminations (and also for nonstoichiometric terminations, see later). All the surfaces energies are converged within $\pm 1\%$, which corresponds to a few mJ/m^2 at most. Even at high number of UO_2 formula units, the surface energy
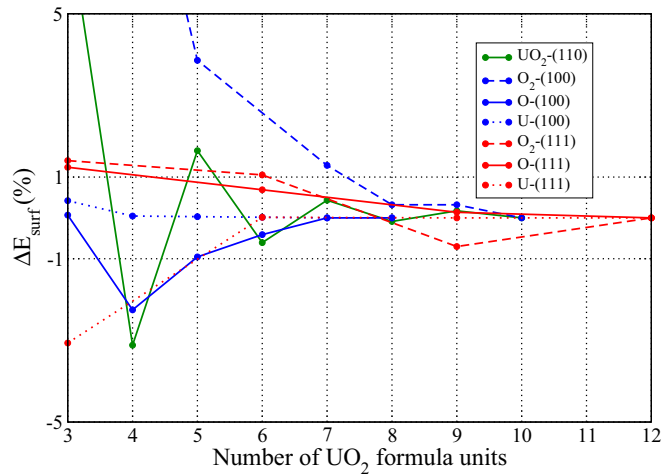
FIG. 5. Convergence of the relative surface energy of the seven terminations of UO$_2$ as a function of the number of UO$_2$ formula units in the slab.

TABLE I. Surface energies of the stoichiometric UO$_2$-(110), O-(100) and O-(111) terminations of UO$_2$ (in J/m^2), as computed by other groups, and compared to present calculations.

Work	Termination		
	O-(111)	UO$_2$-(110)	O-(100)
Classic			
Abramowski *et al.* [24] (Catlow2)	0.89	1.28	1.43
Abramowski *et al.* [24] (Busker)	1.27	2.00	2.81
Tan *et al.* [23]	1.29	2.04	2.85
Boyarchenkov *et al.* [34]	1.14		1.60
Sattonnay *et al.* [22]	1.07	1.72	2.03
Ab initio			
Skomurski *et al.* [28]	0.33	0.83	1.07
Evarestov *et al.* [26]	0.93		
Chaka *et al.* [27]	0.90		
Rabone *et al.* [29]	0.48	0.77	1.25
Rak *et al.* [19]	0.78	1.05	1.47
Bo *et al.* [25]	0.71	1.08	1.49
Tian *et al.* [30]	0.72		
Present work	0.73	1.16	1.46

remains approximately constant indicating that no bias is introduced in the previous equation; i.e., in the bulk energy value $E_{\text{bulk}}^{\text{UO}_2}$.

This type of convergence study has been reported in a large number of recent works. Some of them are performed in the framework of standard DFT. For instance, Skomurski *et al.* [28] found variations of the O-(100), O-(111), and UO$_2$-(110) surface energies larger than 0.1 J/m^2 along their convergence process, with a few of them decreasing irremediably, disclosing a divergence in the calculation method. More recently, Chaka *et al.* [27] observed an equivalent behavior for the (111) termination with a ± 0.1 J/m^2 oscillation. The two last years, some DFT+U calculations using the "U-ramping" or "Occupation Matrix Control" (sometimes without symmetry) reduce this range of variation. Rak *et al.* [19] and Bo *et al.* [25] show a convergence of the O-(100), O-(111), and UO$_2$-(110) surface energies with a few 0.01 J/m^2 of oscillation at the end, whereas Tian *et al.* [30] exhibit a fair behavior of the O-(111) termination with a surface energy converged lower than 0.01 J/m^2.

If all the surface energies computed in this paper are converged up to a few mJ/m^2, their behavior is not the same as a function of the thickness of the slab. The understoichiometric U-(111) and U-(100) terminations are the fastest to converge (see Fig. 5), then the stoichiometric O-(111), O-(100), and UO$_2$-(110) terminations, and lastly, the overstoichiometric O$_2$-(100) and O$_2$-(111) terminations. These latter were the most difficult to minimize, relax and converge, due to their strong modifications of the surface electronic structure, as explained in the following. For a large extent, the process explained in Sec. II C has been brought into play for these terminations.

In Table I, we show the surface energies of the three stoichiometric terminations of the UO$_2$ compound, as computed by other groups and compared to present calculations [using Eq. (1)]. For each result, we retain the surface energy obtained using the largest number of layers within the slab.

First of all, for each work reported in Table I, the surface energies obey the following sequence: $\sigma_{111} < \sigma_{110} < \sigma_{100}$. This is the expected trend for surface energies of compounds with fluorite structure [19]. Even if this "law" is fulfilled in each work, we stress that the spreading of the surface energy values is large for each kind of termination (around 1 J/m^2). This dispersion is not only present in empirical atomistic calculations but also in *ab initio* simulations. Concerning the former, the various forms of interatomic potentials used in these works [22–24,34] are responsible for this scattering. All of these surface energies are far away from present values and sometimes, a few of them, are even two times larger. This strong discrepancy demonstrates that the UO$_2$ terminations are very difficult to describe by means of classical interatomic potentials.

For *ab initio* calculations, a large number of methods and exchange-correlation functionals have been explored these last years: Skomurski *et al.* [28] performed their calculations using the GGA, Evarestov *et al.* [26] used an hybrid functional (with exact exchange), Chaka *et al.* [27] used the GGA and modeled UO$_2$ with the correct AFM **3k** magnetism, Rabone *et al.* [29] used the GGA+U with the U-ramping method, Rak *et al.* [19] used the GGA+U with the U-ramping method and without symmetry, Bo *et al.* [25] used the GGA+U without symmetry, and Tian *et al.* [30] used the GGA+U with the OMC. A reminder that the present work is carried out using the GGA+U functional with the OMC and without symmetry. Rather good agreement is found between present results and the ones obtained by the last three research groups of Table I, with a few tens of mJ/m^2 differences among them. All these works clearly fix the surface energy of the three (111), (110), and (100) terminations as: $\sigma_{111} = 0.7 \pm 0.1$ J/m^2, $\sigma_{110} = 1.1 \pm 0.1$ J/m^2, and $\sigma_{100} = 1.4 \pm 0.1$ J/m^2. We emphasize also that all of these groups perform GGA+U calculations and employ OMC or U-ramping without symmetry. This convergence between state-of-the-art approaches highlights the need to use

sophisticated methods to obtain correct surface energies of UO_2. At odds, strong discrepancies are observed between the first four groups of Tab. I performing *ab initio* calculations and the surface energies estimated by using state-of-the-art approaches. For some cases, several hundreds of mJ/m^2 of differences separate them from the expected result. This large disagreement shows the impossibility to obtain precise UO_2 surface energies without using sophisticated methods.

B. The surface Grand potential

So far, the surface energies are only computed for stoichiometric terminations. In order to evaluate the stability of the nonstoichiometric terminations too, it is needed to go beyond the surface energy formalism, as described in Eq. (1). For this purpose, the surface Grand potential framework is well suited. This one enables the comparison of the thermodynamical stabilities of various terminations with different chemical compositions. We already applied this approach to the PuO_2 terminations [18] and refer the reader to this paper for details. In theory, the surface Grand potential Ω_{surf}^i of the i termination is defined as follows:

$$\Omega_{\mathrm{surf}}^i = \tfrac{1}{2}\big[\Omega_{\mathrm{slab}}^i - N_{\mathrm{UO_2}}\Omega_{\mathrm{bulk}}^{\mathrm{UO_2}}\big]$$

with $N_{\mathrm{UO_2}}$ the number of UO_2 formula units in the slab, Ω_{slab}^i and Ω_{bulk} the Grand potentials of the slab with termination i and of the bulk, respectively. To ensure that the surface is in equilibrium with the bulk UO_2, we also impose that the UO_2 chemical potential obeys:

$$\mu_{\mathrm{UO_2}} = \mu_{\mathrm{U}} + 2\mu_{\mathrm{O}} = E_{\mathrm{bulk}}^{\mathrm{UO_2}}$$

with μ_{U} and μ_{O} the chemical potentials of the uranium and oxygen species in UO_2. By means of these equations, we can deduce the surface Grand potential γ_{surf}^i per surface unit area A:

$$\gamma_{\mathrm{surf}}^i = \frac{\Omega_{\mathrm{surf}}^i}{A} = \phi_{\mathrm{surf}}^i - \alpha^i \Delta\mu_{\mathrm{O}} \qquad \text{with}$$

$$\phi_{\mathrm{surf}}^i = \frac{1}{2A}\left[E_{\mathrm{slab}}^i - N_{\mathrm{U}}E_{\mathrm{bulk}}^{\mathrm{UO_2}} - \frac{E_{\mathrm{mol}}^{\mathrm{O_2}}}{2}(N_{\mathrm{O}} - 2N_{\mathrm{U}})\right]$$

$$\alpha^i = \frac{1}{2A}(N_{\mathrm{O}} - 2N_{\mathrm{U}})$$

with N_{O} and N_{U} the number of oxygen and uranium atoms in each slab i-terminated, and $E_{\mathrm{mol}}^{\mathrm{O_2}}$ the total energy of the O_2 molecule, computed by means of *ab initio* calculations.

The surface Grand potential has no explicit temperature dependance, but this feature can be implicitly taken into account via the oxygen chemical potential. The relative oxygen chemical potential $\Delta\mu_{\mathrm{O}}(p,T)$, as a function of the temperature T and the oxygen partial pressure p, expressed in its ideal gas formulation, reads:

$$\Delta\mu_{\mathrm{O}}(p,T) = \tfrac{1}{2}\big(\mu_{\mathrm{O}}(p,T) - E_{\mathrm{mol}}^{\mathrm{O_2}}\big) \qquad (2)$$

$$= \tfrac{1}{2}\big(\bar{\mu}_{\mathrm{O_2}}(p^0,T) + k_B T \ln(p/p^0)\big) \qquad (3)$$

with p^0 as a reference pressure (here 1 atm) and $\bar{\mu}_{\mathrm{O_2}}(p^0,T)$ includes all the contributions coming from the molecular rotations and vibrations. In the present paper, the latter is not
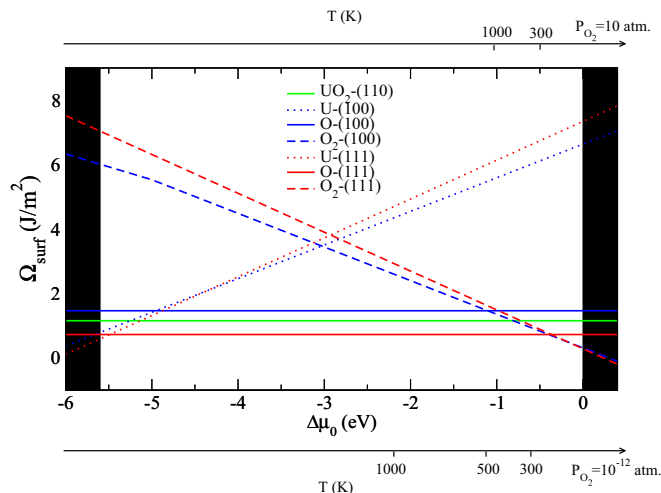

FIG. 6. Surface Grand potentials of seven terminations of UO_2 (in J/m^2) as a function of the relative oxygen chemical potential $\Delta\mu_{\mathrm{O}}$ (in eV): the stoichiometric ones O-(111), O-(100) and UO_2-(110), the overstoichiometric ones O_2-(111) and O_2-(100), and the understoichiometric ones U-(111) and U-(100). For two values of the oxygen partial pressure, a temperature scale is given at the bottom and the top of the figure. The black areas correspond to the limit of stability of the UO_2 compound (-5.6 eV $= -\tfrac{1}{2}E_f^{\mathrm{UO_2}} < \Delta\mu_O$) and of oxygen in condensed matter ($\Delta\mu_O < 0$ eV), with $E_f^{\mathrm{UO_2}}$ the formation energy of the UO_2 compound.

evaluated using first principles calculations, but taken from experimental values, as listed in thermochemical tables [54].

In Fig. 6 we plot the surface Grand potentials of the seven terminations of UO_2. The stoichiometric O-(111), UO_2-(110), and O-(100) terminations are the most thermodynamically stable for oxygen-poor and -intermediary environments, in line with the conclusions found at the level of surface energies. More surprisingly, for oxygen-rich environments, the over-stoichiometric O_2-(111) and O_2-(100) terminations become the most stable. This result would indicate that the overstoichiometry is favored on the surface when this termination is exposed to oxygen-rich environments. Moreover, this starting point would be an interesting candidate in order to create (by diffusion from the surface) overstoichiometric bulk phases such as U_4O_9 and U_3O_8.

However, this stabilization of the O_2-(111) and O_2-(100) terminations is in serious conflict with other results already established in the literature. On one hand, the surface energy sequence $\sigma_{111} < \sigma_{110} < \sigma_{100}$ is no longer fulfilled under oxygen-rich environments since the surface energy of the O_2-(100) becomes lower than the UO_2-(110) one. On the other hand, as stated for a larger number of materials [20,21] and previously shown [18] in the case of PuO_2, this stabilization is not expected since these two terminations are nonstoichiometric and polar. Before answering, we would like to show how this stabilization is different from others already reported in the literature.

Indeed, an unexpected and unphysical stabilization could be inadvertently observed if the strong electronic correlations arising in these materials are not properly taken into account: in a previous work [18], the O_2-(111) and O_2-(100) of PuO_2
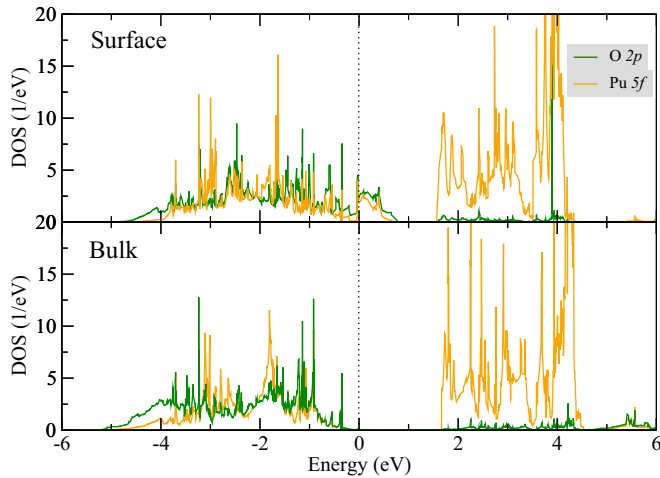
FIG. 7. Electronic density of states of the bulk (bottom) and O$_2$-(100) termination (top) of PuO$_2$. The Fermi level, defined as the VBM for bulk planes, intercepts the valence band of surface planes below the VBM.

were found to be thermodynamically stable in oxygen rich environments when using the GGA-only functional. These terminations were no longer found stable when using the most suited GGA+U framework (see Ref. [18]). This is the reason we claim that a correct treatment of the electronic correlations is needed when one is interested in the thermodynamic stability of polar terminations of correlated materials. In order to heal the polarity, some states have to be filled or emptied at the CBM or at the VBM, respectively. The energetic cost associated with this surface electronic reorganization being related to the band gap value, if the material is treated as a metal or an insulator, the polar termination will be found stable or not, respectively.

In the recent works of Chaka *et al.* [27], and Stubbs *et al.* [31], a strong stabilization of the O$_2$-(111) termination of UO$_2$ is found, in oxygen-intermediary and -rich environments, in qualitative but not quantitative agreement with the present results. This overstabilization is probably related to the electronic correlations that are, at the GGA-only level, not

as well described as within the GGA+U. Indeed, a small band gap (0.38 eV) in the bulk is obtained by these authors, as well as a strong metallization of the termination due to the emptying of two states at the VBM (in order to heal the polarity), and a larger thermodynamical stabilization than the one shown in Fig. 6.

In this paper, we find that the thermodynamic stabilization of the O$_2$-(111) and O$_2$-(100) terminations of UO$_2$ in oxygen-rich environments is not as strong as in the works of Chaka *et al.* [27] and Stubbs *et al.* [31], due to a more relevant treatment of the electronic correlations, described at the GGA+U level. The same terminations are not stabilized at the PuO$_2$ surfaces. In the following, we explain why UO$_2$ and PuO$_2$ are different and why the polarity compensation mechanism through a modification of the surface electronic structure could be efficient for UO$_2$.

C. The electronic structure

The first technique brought into play on the O$_2$-(100) and O$_2$-(111) overstoichiometric terminations is the calculation of the total electronic density of states (DOS). For both, the surface remains insulating. This feature is not expected since two surface electronic states have to be emptied in order to heal the polarity. Generally, such nonstoichiometric polar surfaces become metallic, or at least exhibit an open-shell electronic structure [21,55]. This behavior was previously found on the O$_2$-(100) termination of the PuO$_2$ compound (see Ref. [18] and Fig. 7). To fulfill the polarity compensation criterion, two states are emptied at the VBM. In PuO$_2$, these are **oxygen** states and the surface **oxygen** atom is then reduced.

Concerning the O$_2$-(100) and O$_2$-(111) terminations of UO$_2$, surprisingly, the oxygen surface electronic states are not affected by the polarity compensation. However, the uranium states are strongly modified (see Fig. 8). As for PuO$_2$, to fulfill the polarity compensation criterion, two states have to be emptied at the VBM. However, at odds with PuO$_2$, these ones are now **uranium** states and the surface **uranium** atom is then oxidized.
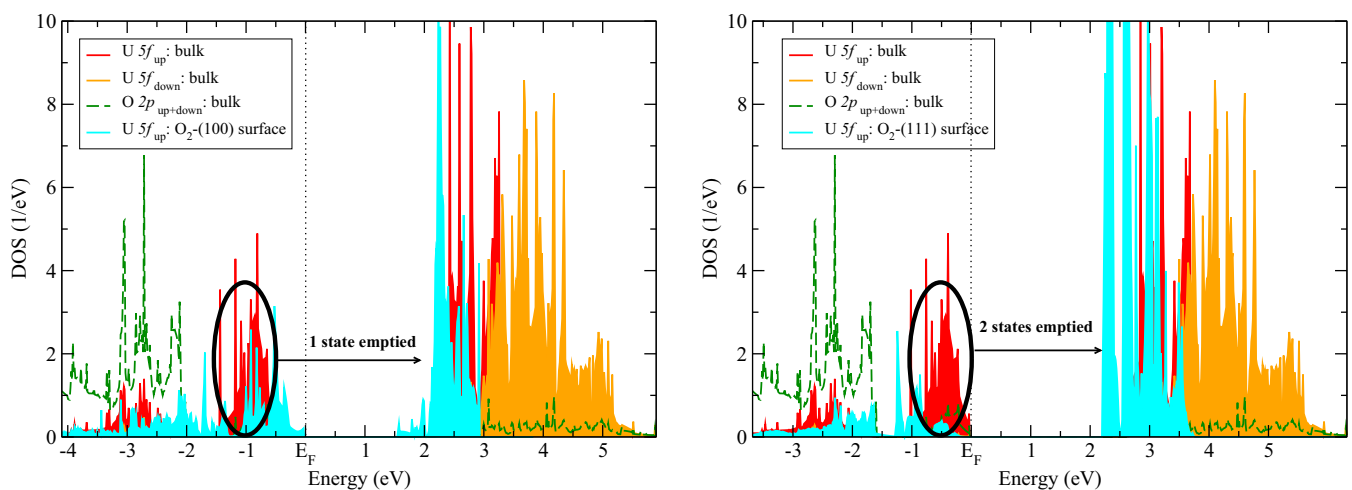

FIG. 8. Left (right) panel: electronic density of states of the O$_2$-(100) (O$_2$-(111)) overstoichiometric terminations, projected on the outermost uranium layer. The Fermi level is defined as the VBM in both cases.

TABLE II. Surface charges of the atoms belonging to the six outermost layers of the UO_2/O_2-(111), UO_2/O_2-(100) and PuO_2/O_2-(111) terminations, computed by means of a Bader topological analysis [56]. "Cation" indicates the layers composed of uranium or plutonium atoms. Within the O_2 layers, the charges carried by each oxygen atom are separated using a "/".

Surface	UO_2/O_2-(111)	UO_2/O_2-(100)	PuO_2/O_2-(111)
O_2	$-0.88/-1.09$	$-1.08/-1.08$	$-0.62/-0.92$
Cation	$+3.08$	$+2.87$	$+2.57$
O_2	$-1.18/-1.24$	$-1.19/-1.19$	$-1.09/-1.17$
Cation	$+2.61$	$+2.86$	$+2.48$
O_2	$-1.31/-1.30$	$-1.25/-1.25$	$-1.25/-1.25$
Cation	$+2.61$	$+2.62$	$+2.49$

TABLE III. Surface charges carried by the atoms belonging to the six outermost layers of the UO_2/O_2-(111), UO_2/O_2-(100) and PuO_2/O_2-(111) terminations in the ionic limit. "Cation" indicates the layers composed of uranium or plutonium atoms. Within the O_2 layers, the charges carried by each oxygen atom are separated using a "/".

Surface	UO_2/O_2-(111)	UO_2/O_2-(100)	PuO_2/O_2-(111)
O_2	O^{2-}/O^{2-}	O^{2-}/O^{2-}	O^-/O^-
Cation	U^{6+}	U^{5+}	Pu^{4+}
O_2	O^{2-}/O^{2-}	O^{2-}/O^{2-}	O^{2-}/O^{2-}
Cation	U^{4+}	U^{5+}	Pu^{4+}
O_2	O^{2-}/O^{2-}	O^{2-}/O^{2-}	O^{2-}/O^{2-}
Cation	U^{4+}	U^{4+}	Pu^{4+}

This behavior is peculiar to a Mott-Hubbard insulator (such as UO_2) and cannot be effective on a common charge-transfer material (such as PuO_2). The f-f band gap of UO_2 leads to a polarity compensation mechanism through the f cationic states and no longer through the p anionic states. Due to the strong electronic correlation effects, the f states emptied at the VBM are shifted up to the upper Hubbard band, leaving the material insulating after healing the polarity, rather than metallic. To our knowledge, this typical feature has never been reported and has to be confirmed for other Mott-Hubbard materials. In the case of UO_2 polar surfaces, we highlight that the polarity compensation through a modification of the surface electronic structure could compete with the most widespread mechanism acting on the surface stoichiometry.

In order to confirm these statements we compute the surface charges by means of a Bader topological analysis [56]. In Table II, we show the charges carried by the atoms belonging to the six outermost layers of the O_2-(111) and O_2-(100) terminations of UO_2 compared to the O_2-(111) termination of PuO_2. Whereas the oxygen atoms are the most affected by the polarity compensation and the plutonium charge remains almost constant within the outermost layers of PuO_2/O_2-(111), the conclusions are reversed in the case of UO_2. The charge of the uranium atoms is strongly modified in the subsurface plane of UO_2/O_2-(111) and deeper concerning the UO_2/O_2-(100) termination. This confirms that the polarity compensation is achieved through the oxygen p states for the O_2-(111) termination of PuO_2 and through the uranium f states for the O_2-(111) and O_2-(100) terminations of UO_2. In the ionic limit, we conclude that the O_2-(111) termination of UO_2 shows one layer with a U^{6+} oxidation state, and the O_2-(100) termination exhibits two layers with a U^{5+} oxidation state. This view, schematized in Table III, is in line with the observations made at the level of the electronic density of states and fulfills the polarity compensation criterion (the sum of the charge of the two or four outermost layers of O_2-(111) or O_2-(100) is equal to +2, respectively).

We also check that the surface atomic structure of the O_2-(111) termination is coherent with the U^{6+} oxidation state. The creation of a short U-O bond on top of the termination ($d_{U-O}^{surf} = 1.8$ Å vs $d_{U-O}^{bulk} = 2.4$ Å) is coherent with the formation of a uranyl group.

It is also interesting to compare UO_2 and PuO_2 concerning the oxidation. Uranium can be easily oxidized, so the emer-

gence of $5+$ and $6+$ oxidation states is not really surprising in an oxygen-rich environment. What is more astonishing is the interplay between (i) the modification of the uranium oxidation state (due to oxidization) and (ii) the compensation of polarity (inherent to the (111) and (100) orientations). This interplay was not possible for PuO_2, since (i) the $5+$ and $6+$ states are not (or hardly) available for plutonium [57–59] and (ii) the states involved in the polarity healing and available at the VBM are no longer cationic but rather oxygen ones. Thus, in the case of the O_2-(111) and O_2-(100) surfaces of PuO_2, the surface oxygen atoms become less reduced (O^-), the plutonium is no longer oxidized and the terminations are not stable.

Lastly, present calculations may be compared to experiments. While one work concerns the (100) surface [60], a large number is dedicated to the (111) termination. Among these latter works, some of them [61,62] do not reveal any oxygen enrichment of the termination, and show a (1×1) reconstruction, meaning that the surface is probably the O-(111) termination defined in this paper and thermodynamically stable in an oxygen intermediary environment (see Fig. 6). A few others [63,64] highlight the formation of an overstoichiometric termination, with additional interstitial oxygen packed into a ($\sqrt{3} \times \sqrt{3}$) R 30° reconstruction. According to authors, this would correspond to the formation of a higher uranium oxide (with a U_3O_7 stoichiometry) which has grown epitaxially onto the surface. Even though we did not consider these types of reconstruction in this paper, this result may be related to the stability of the overstoichiometric O_2-(111) termination in oxygen-rich environment, to some extent. Finally, particular attention may be given to the work performed by Senanayake *et al.* [65]. In their experiments, the (111) termination of UO_2 is cleaned in situ by several cycles of annealing at 800 K and sputtering using Ar^+. They followed by annealing under O_2 at various pressures and times and XPS analysis at 300 K under 10^{-12} atm. in air. They observed the formation of an overstoichiometric termination with a ratio of O/U = 2.22, as previously reported in previous works [63,64]. In addition, they also indicate the reduction of the $5f$ bandwidth, compared to stoichiometric terminations, and interpret this result as the sign of the formation of a more metallic state. We would like to stress that it is exactly the behavior identified in the right panel of Fig. 8. When considering the O_2-(111) termination, the bandwidth of the $5f$ states forming the VBM is reduced,

compared to stoichiometric terminations, due to the emptying of two $5f$ states.

D. The Wulff shape of nanovoids in UO$_2$

A long-standing controversy continues for the Wulff shape of nanovoids in UO$_2$ crystals. An important disagreement still remains between simulations and experiments concerning the surface energy ratio between (100) and (111) terminations. By means of scanning electron microscopy, Castell [32] found that this ratio is equal to $\frac{\sigma_{100}}{\sigma_{111}} = 1.42 \pm 0.05$. This quantity is often discussed [33,34] in order to judge the quality of the surface energy calculations. However, to our knowledge, thus far the Castell ratio has never been approached, where all the previous *ab initio* results have found a ratio within the 1.8–2.0 range. In recent work, Boyarchenkov *et al.* [34] claimed that this ratio can be achieved by classical molecular dynamic simulation, but the surface energies are far from the ones obtained using state-of-the-art *ab initio* techniques (see Section III A). Others have envisaged the hydroxylation of such terminations [19,25,30] showing that the ratio could be obtained at half coverage [33].

In the present study, if we retain the most stable termination for each orientation (see Fig. 6), various situations can be achieved. In oxygen-poor and -intermediary conditions, the O-(111), UO$_2$-(110), and O-(100) terminations are the most thermodynamically stable. The ratio in this case is constant and is equal to exactly 2.0, in line with results obtained previously by other groups. For oxygen-rich environments, these terminations are no longer the most stable. For $-1.0\,\text{eV} < \Delta\mu_O < -0.5$ eV, the surface Grand potential of the O$_2$-(100) terminations becomes lower than the one of the O-(100) termination. At last, for $\Delta\mu_O > -0.5$ eV, the O$_2$-(111) termination is found more stable than O-(111). For $\Delta\mu_O = 0$ eV, the limit of existence of oxygen in condensed matter, the ratio is approximately equal to 1.0.

Consequently, for $-1.0\,\text{eV} < \Delta\mu_O < 0\,\text{eV}$, the ratio is no longer constant and decreases from 2.0 to 1.0. In particular, the exact Castell ratio is obtained for $\Delta\mu_O \approx -0.60\,\text{eV}$ (see Fig. 6). We stress that this value of the relative oxygen chemical potential corresponds to a temperature around 300 K, which is the temperature used in the experiments performed by Castell, irrespective of the oxygen partial pressure. Thus, at ambient temperature, the surfaces of nanovoids (and nanocrystals) would be formed of O-(111) and O$_2$-(100) facets.

IV. CONCLUSIONS

The electronic structure and thermodynamic stability of seven UO$_2$ terminations has been studied by means of *ab initio* GGA+U calculations. Particular attention has been paid to the computation of the electronic structure in order to avoid local minima. In particular, the Occupation Matrix Control used in this work has been deeply detailed. This framework, allowing a correct description of the electronic correlations arising in this material, is proved to be essential in order to correctly describe energetic and electronic properties of UO$_2$ surfaces. The expected surface energy sequence $\sigma_{111} < \sigma_{110} < \sigma_{100}$ is obtained for oxygen-low and -intermediary environments with the polar O-(111), nonpolar UO$_2$, and polar O-(100) terminations, respectively.

In oxygen-rich environments, an unexpected feature is observed: The polar and overstoichiometric O$_2$-(111) and O$_2$-(100) terminations become the most stable. The interplay between the Mott-Hubbard band gap of UO$_2$ and the overstoichiometry of these terminations leads to an peculiar healing of the polarity. In order to fulfill the polarity compensation criterion, some U-$5f$ states (rather than O-$2p$ states) are emptied at the VBM. Undergoing strong correlation effects, these U-$5f$ emptied states are shifted towards the upper Mott band leaving the termination insulating. Taking into account both stoichiometric and overstoichiometric terminations, we show that the 1.42 Castell's ratio can be fulfilled at 300 K in oxygen-rich environments, explaining the Wulff shape of nanovoids in UO$_2$ crystals.

Concerning the unexpected thermodynamic stability of the overstoichiometric terminations in oxygen-rich environments, we stress that the polarity compensation mechanism highlighted in the case of UO$_2$ surfaces is not reported in the literature, to our knowledge. This mechanism shows a strong thermodynamical efficiency with respect to the common mechanism involving a modification of the surface stoichiometry. It would be interesting to study the polar surfaces of other mixed valence compounds with f-f Mott-Hubbard band gap, such as Pu$_2$O$_3$.

[1] P. C. Burns, R. C. Ewing, and A. Navrotsky, Science **335**, 1184 (2012).

[2] W. Ellis, J. Chem. Phys. **48**, 5695 (1968).

[3] B. Campbell and W. Ellis, J. Chem. Phys. **52**, 3303 (1970).

[4] J. Boettger and A. Ray, Int. J. Quantum Chem. **90**, 1470 (2002).

[5] M. N. Hedhili, B. V. Yakshinskiy, and T. Madey, Surf. Sci. **445**, 512 (2000).

[6] The Actinide Research Quarterly : 3rd Quarter 2004, Los Alamos National Laboratory.

[7] P. J. Hay, Mater. Res. Soc. Symp. Proc. **893**, 363 (2006).

[8] P. Carbol, P. Fors, T. Gouder, and K. Spahiu, Geochim. Cosmochim. Acta **73**, 4366 (2009).

[9] T. Gouder, A. Shick, and F. Huber, Top Catal **56**, 1112 (2013).

[10] V. I. Anisimov, J. Zaanen, and O. K. Andersen, Phys. Rev. B **44**, 943 (1991).

[11] A. I. Liechtenstein, V. I. Anisimov, and J. Zaanen, Phys. Rev. B **52**, R5467 (1995).

[12] S.L. Dudarev, A.I. Liechtenstein, M. R. Castell, G. A. D. Briggs, and A. P. Sutton, Phys. Rev. B **56**, 4900 (1997).

[13] S. L. Dudarev, D. N. Manh, and A. P. Sutton, Philos. Mag. B **75**, 613 (1997).

[14] G. Jomard, B. Amadon, F. Bottin, and M. Torrent, Phys. Rev. B **78**, 075125 (2008).

[15] B. Dorado, B. Amadon, M. Freyss, and M. Bertolus, Phys. Rev. B **79**, 235125 (2009).

[16] B. Meredig, A. Thompson, H.A. Hansen, C. Wolverton, and A. van de Walle, Phys. Rev. B **82**, 195128 (2010).

[17] B. Dorado, G. Jomard, M. Freyss, and M. Bertolus, Phys. Rev. B **82**, 035114 (2010).

[18] G. Jomard and F. Bottin, Phys. Rev. B **84**, 195469 (2011).

[19] Z. Rak, R. Ewing, and U. Becker, Surf. Sci. **608**, 180 (2013).

[20] C. Noguera, J. Phys.: Condens. Matter **12**, R367 (2000).

[21] J. Goniakowski, F. Finocchi, and C. Noguera, Rep. Prog. Phys. **71**, 016501 (2008).

[22] G. Sattonnay and R. Tétot, J. Phys.: Condens. Matter **25**, 125403 (2013).

[23] A. H. Tan, R. W. Grimes, and S. Owens, J. Nucl. Mater. **344**, 13 (2005).

[24] M. Abramowski, R. W. Grimes, and S. Owens, J. Nucl. Mater. **275**, 12 (1999).

[25] T. Bo, J.-H. Lan, Y.-L. Zhao, Y.-J. Zhang, C.-H. He, and Z.-F. Chai, J. Nucl. Mater. **454**, 446 (2014).

[26] R. Evarestov, A. Bandura, and E. Blokhin, Acta Mater. **57**, 600 (2009).

[27] A. M. Chaka, G. A. Oxford, J. E. Stubbs, P. J. Eng, and J. R. Bargar, Computational and Theoretical Chemistry **987**, 90 (2012).

[28] F. Skomurski, L. Shuller, R. Ewing, and U. Becker, J. Nucl. Mater. **375**, 290 (2008).

[29] J. Rabone and M. Krack, Comput. Mater. Sci. **71**, 157 (2013).

[30] X. feng Tian, H. Wang, H. xing Xiao, and T. Gao, Comput. Mater. Sci. **91**, 364 (2014).

[31] J. E. Stubbs, A. M. Chaka, E. S. Ilton, C. A. Biwer, M. H. Engelhard, J. R. Bargar, and P. J. Eng, Phys. Rev. Lett. **114**, 246103 (2015).

[32] M. R. Castell, Phys. Rev. B **68**, 235411 (2003).

[33] M. Abramowski, S. E. Redfern, R. W. Grimes, and S. Owens, Surf. Sci. **490**, 415 (2001).

[34] A. Boyarchenkov, S. Potashnikov, K. A. Nekrasov, and A. Y. Kupryazhkin, J. Nucl. Mater. **421**, 1 (2012).

[35] P. Hohenberg and W. Kohn, Phys. Rev. **136**, B864 (1964).

[36] W. Kohn and L. J. Sham, Phys. Rev. **140**, A1133 (1965).

[37] The present results have been obtained through the use of the ABINIT code, a common project of the Université Catholique de Louvain, Corning Incorporated, and other contributors, see the URL http://www.abinit.org.

[38] X. Gonze, B. Amadon, P.-M. Anglade, J.-M. Beuken, F. Bottin, P. Boulanger, F. Bruneval, D. Caliste, R. Caracas, M. Côté *et al.*, Comput. Phys. Commun. **180**, 2582 (2009).

[39] P. E. Blöchl, Phys. Rev. B **50**, 17953 (1994).

[40] M. Torrent, F. Jollet, F. Bottin, G. Zerah, and X. Gonze, Comput. Mater. Sci. **42**, 337 (2008).

[41] J. P. Perdew, K. Burke, and M. Ernzerhof, Phys. Rev. Lett **77**, 3865 (1996).

[42] M. A. L. Marques, M. J. T. Oliveira, and T. Burnus, Comput. Phys. Commun. **183**, 2272 (2012).

[43] G. Jomard, F. Bottin, and G. Geneste, J. Nucl. Mater. **451**, 28 (2014).

[44] M. Torrent, N. A. W. Holzwarth, F. Jollet, D. Harris, N. Lepley, and X. Xu, Comput. Phys. Commun. **181**, 1862 (2010).

[45] F. Bottin, S. Leroux, A. Knyazev, and G. Zérah, Comput. Mater. Sci. **42**, 329 (2008).

[46] B. Amadon, F. Jollet, and M. Torrent, Phys. Rev. B **77**, 155104 (2008).

[47] B. Dorado, M. Freyss, B. Amadon, M. Bertolus, G. Jomard, and P. Garcia, J. Phys.: Condens. Matter **25**, 333201 (2013).

[48] M. Idiri, T. LeBihan, S. Heathman, and J. Rebizant, Phys. Rev. B **70**, 014113 (2004).

[49] Y. Baer and J. Schoenes, Solid State Commun. **33**, 885 (1980).

[50] J. Killeen, J. Nucl. Mater. **88**, 185 (1980).

[51] P. Santini, R. Lemanski, and P. Erdos, Adv. Phys. **48**, 537 (1999).

[52] H. J. Monkhorst and J. D. Pack, Phys. Rev. B **13**, 5188 (1976).

[53] F. Zhou and V. Ozolins, Phys. Rev. B **83**, 085106 (2011).

[54] D. R. Lide, ed., *CRC Handbook of Chemistry and Physics* (CRC press LLC, Boca Raton, 1998), 79th ed.

[55] F. Bottin, F. Finocchi, and C. Noguera, Phys. Rev. B **68**, 035418 (2003).

[56] R. Bader, Chem. Rev. **91**, 893 (1991).

[57] J. M. Haschke, T. H. Allen, and L. A. Morales, Science **287**, 285 (2000).

[58] L. Petit, A. Svane, Z. Szotek, and W. M. Temmerman, Science **301**, 498 (2003).

[59] P. A. Korzhavyi, L. Vitos, D. A. Andersson, and B. Johansson, Nat. Mater. **3**, 225 (2004).

[60] C. Muggelberg, M. Castell, G. Briggs, and D. Goddard, App. Surf. Sci. **142**, 124 (1999).

[61] M. Castell, S. Dudarev, C. Muggelberg, A. Sutton, G. Briggs, and D. Goddard, J. Vac. Sci. Technol. A **16**, 1055 (1998).

[62] S. L. Dudarev, M. R. Castell, G. A. Botton, S. Y. Savrasov, C. Muggelberg, G. A. D. Briggs, A. P. Sutton, and D. T. Goddard, Micron **31**, 363 (2000).

[63] M. Castell, C. Muggelberg, S. Dudarev, A. Sutton, G. Briggs, and D. Goddard, Appl. Phys. A **66**, S963 (1998).

[64] C. Muggelberg, M. R. Castell, G. A. D. Briggs, and D. T. Goddard, Surf. Rev. Lett. **05**, 315 (1998).

[65] S. D. Senanayake and H. Idriss, Surf. Sci. Spectra **13**, 72 (2006).